JOURNAL OF Materials CHEMISTRY

# Growth of calcium phosphate onto coagulated silica prepared by using modified simulated body fluids

**Juan Coreño,[a] Rogelio Rodríguez,*[a,b] Miguel A. Araiza[c] and Victor M. Castaño[b]**

[a] *Departamento de Física, Universidad Autónoma Metropolitana-Iztapalapa, Apdo. Postal 55-534, México, D.F. 09340*
[b] *Instituto de Física, Universidad Nacional Autónoma de México, Apdo. Postal 1-1010, Querétaro, Qro. México 76001*
[c] *Facultad de Odontología, Universidad Nacional Autónoma de México, Ciudad Universitaria, México, D.F. 04510*

***Received 11th May 1998, Accepted 25th September 1998***

Silica sols prepared by the alkaline hydrolysis of tetraethylorthosilicate were coagulated by adding an excess of a $CaCl_2$ aqueous solution. The aggregates were immersed into three different modified simulated body fluids at 90 °C to allow the growth of a calcium phosphate phase onto the silica aggregates. The apatite phase grew faster compared to previous studies. Also, the amount of the crystalline apatite yield was higher when the simulated body fluid employed had the largest Ca/P ratio, as measured by X-ray diffraction. The relevance of these findings is discussed in terms of the current and future trends in biomaterials research and development.

## Introduction

The preparation of synthetic biomaterials, aimed to be employed for prosthestic applications in living organisms, has attracted growing interest in the last few decades. For instance, apatite coatings have been applied onto different substrates to produce a number of interesting materials with potential biomedical applications.[1] The development of novel nanocomposites opens a broad new field of research since, in principle, it is possible to control, to a great extent, the corresponding morphology, which in turn is related to the biomedical and physical properties.[2]

A number of important requirements, in addition to the obvious biocompatibility, ought to be fulfilled if synthetic materials are to be used for human applications. In fact, one of the most important characteristics is the corresponding porous structure, since the extra-cellular fluids must be allowed to flow through the inner structure of the biomedical device to allow an adequate osteoconduction.[3,4]

Among the materials that are known to have an appropriate biological activity when implanted in living organisms calcium phosphates deserve special attention.[5] Historically speaking, the modern use of these materials for bone repair was probably pioneered by Albee in the 1920s[6] which are, nowadays, widely employed for low-loading hard tissue repair and augmentation of living bone.[4] The excellent histological behaviour of these materials, either synthetic or natural, is attributed to their chemical similarity to the mineral phase of natural bone, hydroxyapatite [$Ca_{10}(PO_4)_6(OH)_2$] or HAp, which is the classical example. In fact, the crystallographic and chemical properties of HAp closely resemble those of bone and tooth minerals.[7]

Bioactive glasses have also been used for implants because these materials bond to bone through an intervening bone-like apatite layer formed on their surfaces in a living body-like environment.[5,8] Interestingly this apatite layer is calcium-deficient compared with hydroxyapatite, being formed by small crystallites and containing small amounts of carbonate.[9] In $CaO–SiO_2$-based bioactive glasses,[10] it has been found that silica forms a low solubility matrix in which the network of silicate chains acts as a framework for ionic species ($Ca^{2+}$, $PO_4^{3-}$, $Na^+$, *etc.*), whose role is to stimulate the biochemical environment surrounding the bioactive glass.

A hydrated silica gel layer is formed on the glass surface and provides favorable sites for apatite nucleation. It has been suggested in the literature[11] that, in contrast to dense silica, this silica layer produced on the bioglasses, is flexible enough to provide the oxide–oxide spatial requirements to match the bone lattice, thus providing epitaxial sites for bone growth.

The potential role of hydrated silica species on biological mineralization[9] also points out the relevance of producing materials with high surface areas, controlled porosity and appropriate chemical groups available for the desired interactions. One possible approach is the coating of different substrates with biocompatible apatite layers, by using various techniques, which range from standard vacuum evaporation to chemical vapor deposition (CVD) technologies. Unfortunately, long-term animal studies suggest that the HAp coatings may degrade or come off.[9]

One interesting method to produce calcium phosphate apatites at low temperature is through the immersion of silica gels into simulated body fluid (SBF).[12–17] Besides the promising potential applications of these experiments, from a practical standpoint, the available reports in the literature reveal a very low reaction kinetics and a limitation on the number of available surface chemical groups for the reaction with the surrounding SBF, since the silica gels reportedly employed only react on the areas exposed to the SBF. Accordingly, an alternative method, by starting from silica sols rather than gels, which are coagulated *in situ* by adding controlled amounts of calcium ions, and by using three different modified SBFs, is reported here. The higher temperature of reaction, namely 90 °C, makes the available reacting chemical groups more reactive; additionally, due to the use of nanometer-sized sols and to the coagulation process, one can obtain faster reaction times, higher yields and more controllable conditions compared with previous studies.

## Experimental

Coagulated silica was obtained by preparing pure silica sol by the sol–gel method under alkaline conditions of the hydrolysis reaction, followed by a coagulation procedure of the silica particles through the addition of an excess of calcium chloride. It is important to point out that, unlike previous reports in

the literature, in the present studies, coagulated silica sols were employed instead of the standard silica gels.

### Sol preparation

A solution of 4 moles of distilled water in 6 moles of ethanol (reactive grade)(Baker Co.) was added to another solution of 1 mole of tetraethylorthosilicate (TEOS) (Aldrich Chem. Co.) in 6 moles of ethanol, under vigorous stirring. The starting pH of water was adjusted to 12 by using $NH_4OH$. The resulting mixture was poured into a round double-necked flask, and heated to reach reflux conditions. A profile of the silica particle size as a function of the reaction time was obtained by sampling at regular time intervals by using dynamic light scattering techniques. Once a constant particle diameter was obtained, the sol–gel reaction was stopped by diluting with ethanol and cooling the system to prevent gelation. Silica sols prepared under these (basic) conditions are electrically stabilized; consequently, they can be coagulated at will by the addition of a suitable salt.

### Sol coagulation

An aqueous 0.1 M $CaCl_2$ solution was added dropwise to a fixed volume of colloidal silica suspension under stirring; the final concentration of calcium ions was 0.01 M. After stirring for one hour, the flocculate was allowed to settle under the influence of gravity; the liquid was decanted and the solid centrifuged. The solid part was washed twice by resuspending it in distilled water and stirring gently for 20 min. The coagulates were dried at 400 °C for 2 days and ground by using an agate mortar.

### Calcium–phosphates growth

The growth of calcium phosphate crystals was achieved by resuspending the silica coagulates in an aqueous solution containing calcium and phosphate ions. Four different ionic solutions were used:

1) SBF at 37 °C

2) mSBF-1.0: modified SBF with Ca/P = 1.00 at 90 °C

3) mSBF-1.7: modified SBF with Ca/P = 1.67 at 90 °C

4) mSBF-2.5: modified SBF with Ca/P = 2.50 at 90 °C

Table 1 summarizes the ionic composition for the four SBF solutions; human plasma is also reported for comparison purposes.

Each experiment using mSBF was carried out in three round flasks. The first flask contains only 20 ml of mSBF, to rule out a possible spontaneous crystallization. The second flask contains 0.35 g of 0.125–0.25 mm ground silica in 30 ml of mSBF and the third contains 0.20 g of coagulated silica ground to sizes smaller than 0.125 mm in 20 ml of mSBF. The third flask was sampled on a regular basis to measure phosphate concentration in the solution as a function of time and to obtain X-ray diffractograms of the corresponding products.

The experiment at 37 °C was taken as reference. In this case, the silica aggregates were used without previous drying. They were added to the SBF and kept at 37 °C under agitation for 9 days. After this period the solid was washed and dried at 100 °C for 2 h.

SBF and mSBFs solutions were prepared by dissolving, at different concentrations, reagent grade NaCl, $NaHCO_3$, KCl, $Na_2HPO_4{\cdot}12H_2O$, $MgCl_2{\cdot}H_2O$, $CaCl_2$ or $Na_2SO_4$, buffered at pH = 7.4 by using tris(hydroxymethyl)aminomethane [$(CH_2OH)_3CNH_2$] and hydrochloric acid.

### Characterization techniques

The dynamic light scattering (DLS) apparatus used to measure the particle size was a Brookhaven Instrument with a digital correlator model 9000; in all cases the scattering angle was set to 90°, the measurements were done at room temperature and the light source was an argon ion laser operating at 488 nm. The phosphate concentration was measured by the molybdenum blue method[18] using a UV–VIS absorption spectrophotometer (Perkin Elmer Lambda 5) at 690 nm. The X-ray diffractograms (XRD) of the samples were obtained in a Phillips diffractometer in the range 20–50° with a scanning rate of 2° $min^{-1}$. Scanning electron microscopy (SEM) was carried out in a Zeiss model DSM940A; all samples were finely ground and carbon-coated. μ-Raman characterization was carried out in a DILOR apparatus model Labram equipped with a He–Ne laser as a light source and a confocal optical microscope; the wavenumber range of the scattered light was varied from 100 to 1200 $cm^{-1}$. $^{31}P$ NMR spectra were taken on a Bruker ASX300 NMR spectrometer using a 4 mm CP MAS probe at 5 kHz. $H_3PO_4$ was used as reference.

## Results and discussion

Fig. 1 shows the X-ray diffraction pattern corresponding to pure HAp where the plane indices of the main reflections are shown. XRD for pure silica, prior to the immersion into the mSBF and with the same thermal treatment as all samples, was also obtained (not shown); for this sample no crystalline reflections were observed but only a broad peak around 23° due to the amorphous phase.

XRD for samples containing calcium phosphate grown on their surfaces at different immersion times in different mSBFs are shown in Fig. 2–4. Fig. 2 corresponds to the diffractograms

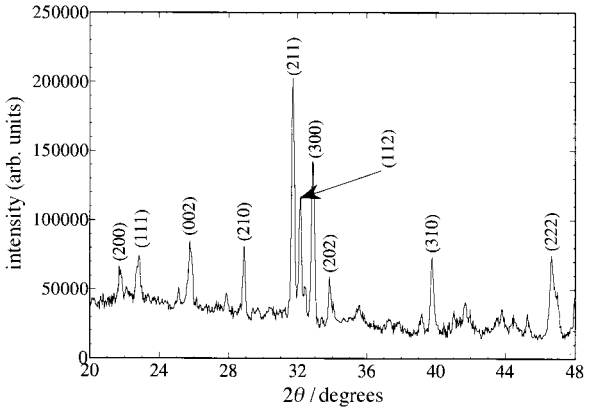


**Fig. 1** X-Ray diffractogram of pure crystalline hydroxyapatite.

**Table 1** Ion concentration of standard blood plasma, SBF, and the modified SBF used for calcium phosphates growth onto silica aggregates

| Ion concentration/mM | Ca/P | $Na^+$ | $K^+$ | $Ca^{2+}$ | $Mg^{2+}$ | $Cl^-$ | $HCO_3^-$ | $HPO_4^{2-}$ | $SO_4^{2-}$ |
|---|---|---|---|---|---|---|---|---|---|
| Blood plasma | 2.5 | 142.0 | 5.0 | 2.5 | 1.5 | 103.0 | 27.0 | 1.0 | 0.5 |
| SBF | 2.5 | 142.0 | 5.0 | 2.5 | 1.5 | 147.0 | 4.2 | 1.0 | 0.5 |
| Modified SBF, No. 1 | 1.67 | 142.4 | — | 2.0 | — | 144.0 | — | 1.2 | — |
| Modified SBF, No. 2 | 1.0 | 143.0 | — | 1.5 | — | 143.0 | — | 1.5 | — |
| Modified SBF, No. 3 | 2.5 | 142.0 | — | 2.5 | — | 145.0 | — | 1.0 | — |

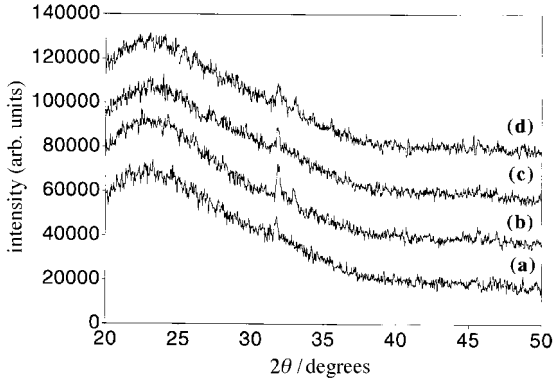


**Fig. 2** X-Ray diffractograms of samples immersed in mSBF with Ca/P = 1.0 at 90 °C and different immersion times: (a) 10 h, (b) 23 h, (c) 33 h and (d) 48 h.

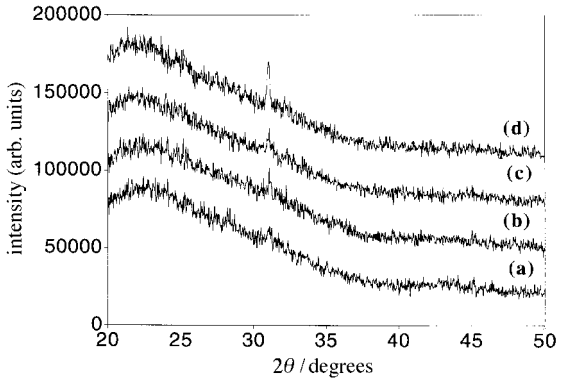


**Fig. 3** As for Fig. 2 but for samples immersed in mSBF with Ca/P = 1.67.

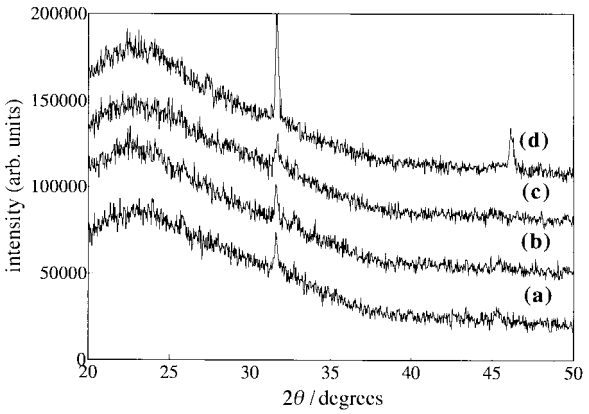


**Fig. 4** As for Fig. 2 but for samples immersed in mSBF with Ca/P = 2.5.

of the samples immersed in mSBF-1.0 at 90 °C for 10, 23, 33 and 48 h, respectively. The whole set of reflections for the crystalline phase is difficult to obtain since it is the minor component of the resulting material (*ca.* 10%). It is worth mentioning that, since the apatite growth takes place on the surface of small coagulated silica particles, the silanol groups on their surfaces and the open structure produced by the coagulating process allow the coating to be both internal and external, unlike the methods which use silica gels; this means that the reflections may also contain contributions from the internal coating. Since the reaction conditions favor apatite formation,[10] the characteristic reflection for the crystalline phase is located around 32°; this peak is assigned to an overlap of the diffraction bands of three crystalline spacings: (211), (112) and (300) according to the literature.[19] Fig. 3 and 4 are

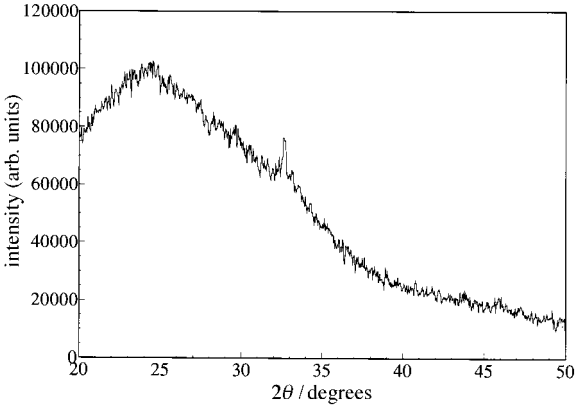


**Fig. 5** X-Ray diffractogram of a sample prepared at 37 °C immersed in SBF for 7 days.

equivalent to Fig. 2 but using mSBF-1.7 and mSBF-2.5, respectively. For comparison purposes, the diffractogram for the experiment at 37 °C is shown in Fig. 5.

The diffractograms of Fig. 2–4 show, in addition to the contribution of the amorphous silica, the crystalline reflection corresponding to the apatite phase. As the Ca/P ratio in the mSBFs was increased, the intensity of the reflection was also increased. This is clearly observed in Fig. 6 where the intensity of the characteristic apatite peak is plotted as a function of the immersion time for the three different mSBFs. This plot shows that, at the beginning of the crystal growth on the silica surface, the amount of the crystalline phase is small, corresponding to an induction period where the silica surface offers multi-nucleating sites where the apatite can grow. Up to 33 h the amount of crystals remains practically constant as revealed by the intensity of the reflection, which is nearly the same as after induction. However, after this time, for Ca/P ratios of 1.67 and 2.5, their heights have increased producing sharper and stronger X-ray reflections. Since the height of the diffraction peak is known to be proportional to the amount of crystals which contribute to the peak, there is a 2.2 fold increase in this crystal content for mSBF-2.5 compared with mSBF-1.0. It is important to mention that these growth times are considerably shorter than typical HAp formation periods reported previously.[19]

μ-Raman spectra were obtained for all samples and pure HAp. The Raman spectrum for pure HAp is shown in Fig. 7(a), while the sample with Ca/P 2.5 is shown in Fig. 7(b) where it is possible to observe a small signal corresponding to the apatite superimposed on a strong fluorescence signal produced by the silica substrate. As before, only the strongest apatite band at 962 $cm^{-1}$ due to the phosphate symmetric stretching vibration[20] is observed because this phase represents only a small percentage of the resulting material. Similar

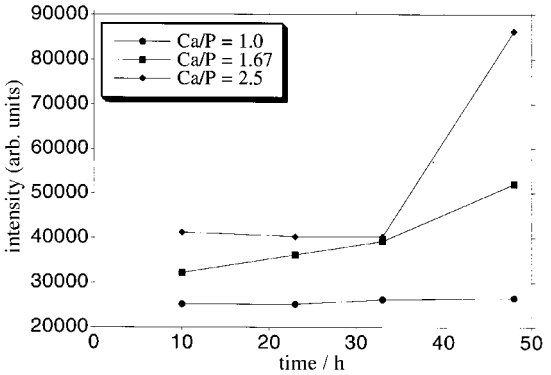


**Fig. 6** Plot of the 32° reflection intensity as a function of the immersion time for samples immersed in the three mSBFs.

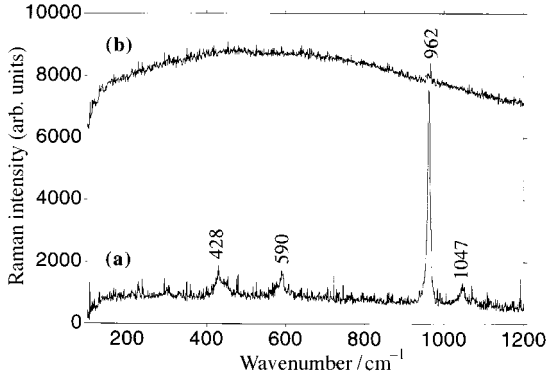


**Fig. 7** μ-Raman spectra of pure HAp (a) and for the sample Ca/P 2.5 immersed in mSBF for 48 h.

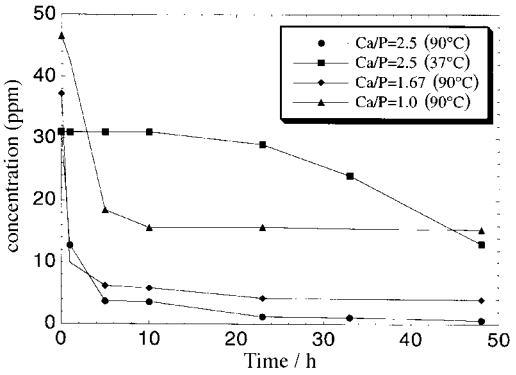


**Fig. 10** Consumption of phosphorus as a function of time for all experiments.

spectra (not shown) were obtained for the remainder of the samples.

Fig. 8 and 9 show the $^{31}$P MAS NMR spectra for pure HAp and for the sample immersed in mSBF-2.5 for 48 h, respectively. In Fig. 9 only one $^{31}$P resonance with weak sidebands is observed. The isotropic chemical shifts obtained are $\delta$ 2.710 for pure HAp and $\delta$ 2.924 for the sample. These values are in accord with the chemical shift reported for calcium phosphate

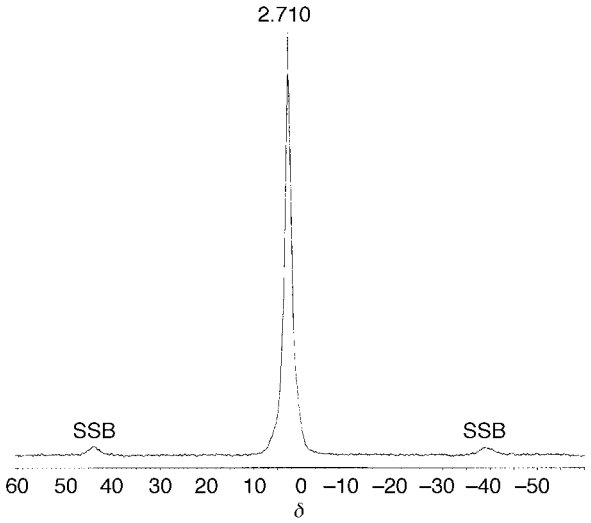


**Fig. 8** $^{31}$P MAS NMR spectrum of pure hydroxyapatite.

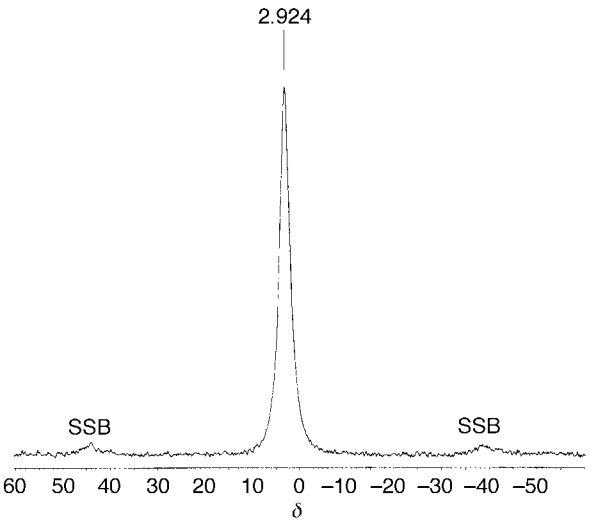


**Fig. 9** $^{31}$P MAS NMR spectrum of the sample Ca/P 2.5 immersed in mSBF for 48 h.

apatites with Ca/P ranging from 1.14 to 1.66 ($\delta$ 2.8$\pm$0.2) which is clearly different from those corresponding to other calcium phosphates.[21] This result confirms the identification of the crystalline phase formed as apatite.

Fig. 10 shows the change in P concentration for the four experiments. Both the rate and the amount of P consumption are similar for all the three experiments at 90 °C. The decrease in P concentration for these experiments ends approximately 23 h after the beginning of the reaction, whereas for the experiment at 37 °C, it starts approximately at this point. It is interesting that, even for the experiment at 37 °C, which corresponds to the slowest apatite growth, an apatite growth rate faster than those reported for gels dried at 400 °C is observed.[19] There are a number of factors which explain this behavior: (a) the present experiments were carried out using coagulated silica sols instead of the standard gels, which increases the active surface area available for the chemical reaction, (b) the higher temperature of reaction makes the available chemical groups more reactive so reducing the reaction time. Additionally, the Ca ions adsorbed on the silica sol may favour the growth of the apatite phase by increasing the ionic activity of the surrounding solution near the flocs. It is important to mention that, for the series of experiments without silica sols (*i.e.*, containing only mSBF), there was no P consumption during the same time intervals reported here.

SEM micrographs for the whole set of samples are shown in Fig. 11–15. Fig. 11 reveals a smooth surface corresponding to pure silica. The micrographs shown in Fig. 12–14 correspond to experiments where the apatite grew onto

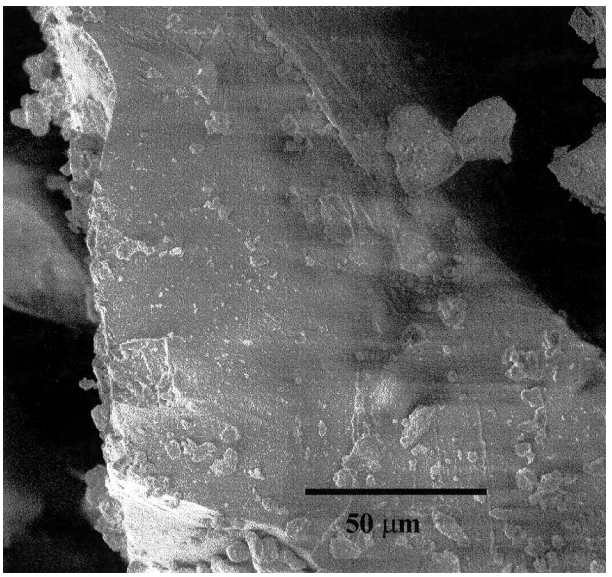


**Fig. 11** SEM micrograph of pure silica.

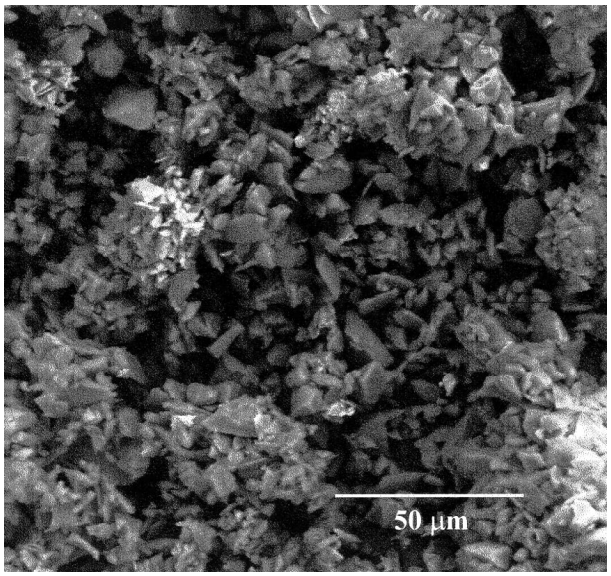


**Fig. 12** SEM micrograph from a sample with Ca/P = 1.67 for an immersion time of 48 h.

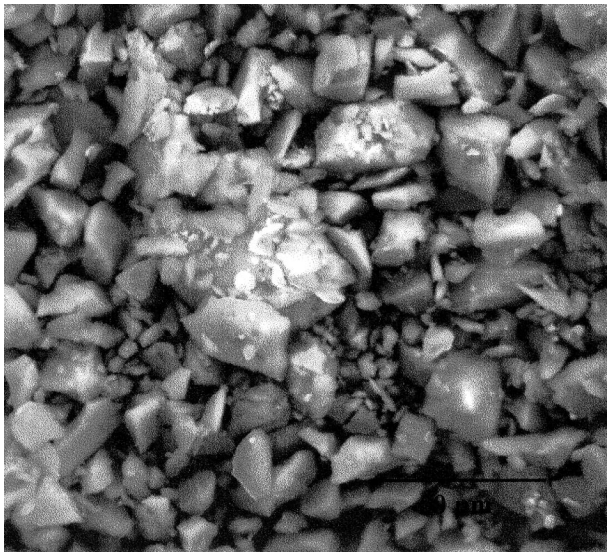

**Fig. 13** SEM micrograph from a sample with Ca/P = 2.5 for an immersion time of 48 h.

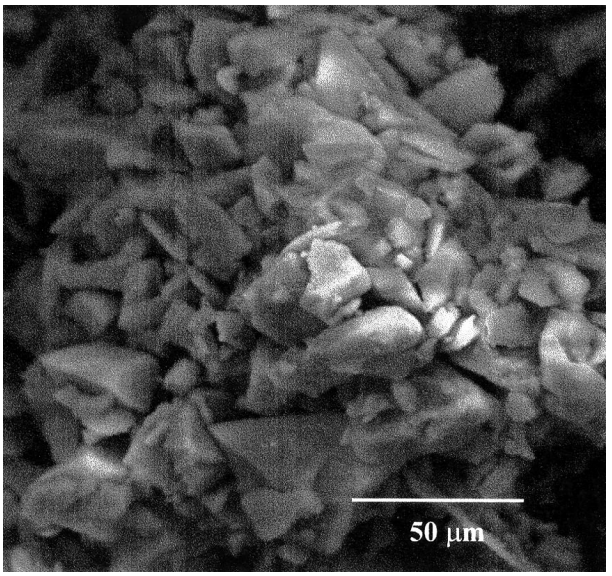


**Fig. 14** SEM micrograph from a sample with Ca/P = 1.0 for an immersion time of 48 h.

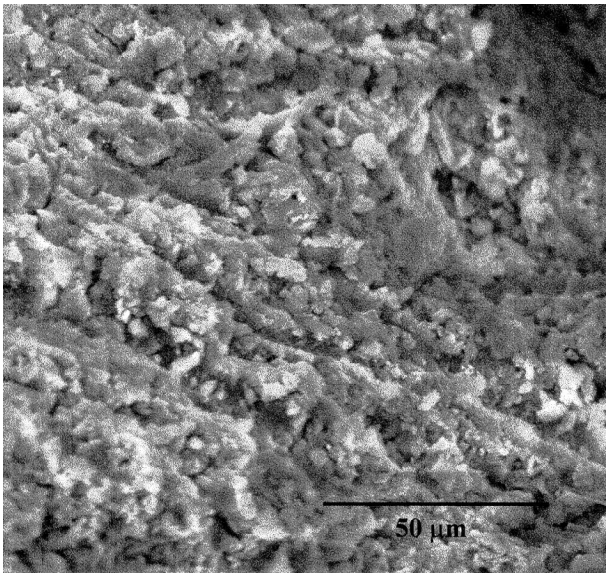


**Fig. 15** SEM micrograph from a sample at 37 °C and 7 days immersion in SBF.

0.125–0.25 mm ground silica particles at 90 °C during 48 h. These do not show the typical spherical morphology that has been observed in similar work at 37 °C.[14,19]

Fig. 12 shows the micrograph corresponding to samples immersed in mSBF-1.7; this shows smaller and more uniform crystallite sizes (*ca.* 12 μm) with respect to the other two experiments at different Ca/P ratios. Fig. 13 shows a micrograph corresponding to Ca/P = 2.5 where the apatite crystals form a loose cluster with a wider particle size distribution compared with Fig. 12. These characteristics are not observed in Fig. 14 (Ca/P = 1.0) where the crystals in the aggregate are tightly distributed.

For comparison, the micrograph for the experiment at 37 °C is shown in Fig. 15. Here, it can be seen that this rough surface is quite different from the other SEM micrographs. The apatite phase shows smaller and poorly defined crystallites, compared with samples at 90 °C. This sample was kept in the SBF until XRD characteristic peaks were observed (after 7 days). These results demonstrate the strong influence of temperature on the growth of the crystalline phase.

For apatite growth onto silica fired at 400 °C[22] it has been reported that the morphology is Ca/P dependent, and can be modified by the presence of some ions. In this work it is observed that the Ca/P ratio affects both the crystal size and the way they cluster together, but not significantly the crystal morphology. It seems that the effect of Ca/P ratio on the crystal morphology is diminished at the higher temperature employed for the apatite growth.

It is interesting to note the dependence of the apatite morphology on the nature of the substrate. In this work, the sample prepared in SBF at 37 °C does not show the flake-like crystals reported when fired silica was used,[22] but rather a uniformly distributed crystal layer without a defined morphology. Also, this layer was grown more rapidly than that previously reported.[19] These observations can be explained by the greater silanol density present in a wet coagulated silica sol, compared with fired silica, since it has been proposed that silanol groups are responsible for apatite nucleation.[11]

All the above results demonstrate that the silica is covered with a layer of apatite whose morphology depends on temperature, immersion time and the type of substrate. The morphology of this nano-composite can also be modified, either

by changing the Si:Ca/P ratio, or by modifying the route of adding the constituents.

One important advantage of the present approach over the previous reports is that, since the silica sol was coagulated, the active sites suitable for apatite growth are evenly distributed over the whole sample surface, consequently it is expected that the crystalline phase will grow both inwardly and outwardly on the silica flocs. This shows the clear advantage of using sols rather than gels to allow the presence of more active groups available for the corresponding reaction. Additionally, by choosing the appropriate starting silica particle size it is possible to control the porosity and the interstitial volume of the material. The immersion time, and, in turn, the thickness of the HAp layers, also slightly modifies the average pore size.

## Conclusions

A novel composite material with potential biomedical applications prepared by coagulating silica sols with calcium ions, is reported. With this procedure, a silica substrate covered inwardly and outwardly with a crystalline apatite phase can be produced. The role of the liquid phase (SBF) was analyzed by using several modified simulated body fluids. The kinetics of each process is certainly an area worth further study, not only because of its relevance for the production of novel biomaterials, but also because it opens the possibility of preparing other ceramic-like systems at low temperature.

## Acknowledgments

The authors are indebted to Ing. Francisco Rodríguez Melgarejo from CINVESTAV, Querétaro and to Dra. Antonieta Mondragón from IFUNAM, for their valuable assistance in the Raman measurements.

## References

1 K. A. Khor, P. Cheang and Y. Wang, *JOM*, 1997, **49**, 51.
2 R. Rodríguez, J. Coreño and V. Castaño, *Adv. Comp. Lett.*, 1996, **5**, 25.
3 L. L. Hench and J. Wilson, *Science*, 1984, **226**, 630.
4 F. H. Albee, *Ann. Surg.*, 1920, **71**, 32.
5 R. Z. LeGeros, *Calcium Phosphates in Oral Biology and Medicine*, Karger, Basel, Switzerland, 1991.
6 K. de Groot, in *Contemporary Biomaterials*, ed. J. W. Boretos and M. Eden, Noyes Publications, Park Ridge, NJ, 1984, pp. 477–492.
7 R. H. Doremus, *J. Mater. Sci.*, 1992, **27**, 285.
8 M. M. Pereira, A. E. Clark and L. L. Hench, *J. Am. Chem. Soc.*, 1995, **18**, 2463.
9 L. L. Hench, *J. Am. Ceram. Soc.*, 1991, **74**, 1487.
10 L. L. Hench and A. E. Clark, *Biocompatibiity of Orthopedic Implants*, ed. E. F. Williams, CRC Press, Boca Raton, FL, 1982, vol. 2, pp. 129–170.
11 L. L. Hench and E. C. Ethridge, *Biomaterials: An Interfacial Approach*, *Biophysics and Bioengineering Series*, ed. A. Noordergraaf, Academic Press, New York, 1982, vol. 4, p. 139.
12 A. Ravaglioli and A. Krajewski, *Bioceramics: Materials, Properties and Applications*, Chapman & Hall, London, 1992, pp. 140 and 175.
13 T. J. Kokubo, *J. Non-Cryst. Solids*, 1990, **120**, 138.
14 P. Li, C. Ohtsuki, T. Kokubo, K. Nakanishi, N. Soga, T. Nakamura and T. Yamamuro, *J. Am. Ceram. Soc.*, 1992, **75**, 2094.
15 T. Kokubo, *Biomaterials*, 1991, **12**, 1155.
16 R. Fresa, A, Constantini, A. Buri and F. Branda, *J. Non-Cryst. Solids*, 1995, **16**, 1249.
17 M. Tanahashi, T. Kokubo, T. Nakamura, Y. Katsura and M. Nagano, *J. Non-Cryst. Solids*, 1996, **17**, 47.
18 C. Sung-Baek, N. Kazuki, T. Kokubo, N. Soga, C. Ohtsuki, T. Nakamura, T. Kitsugi and T. Yamamuro, *J. Am. Ceram. Soc.*, 1995, **78**, 1769.
19 P. Li, C. Ohtsuki, T. Kokubo, K. Nakanishi, N. Soga, T. Nakamura and T. Yamamuro, *J. Mater. Sci. Mater. Med.*, 1993, **4**, 127.
20 M. A. Walters, Y. C. Leung, N. C. Blumenthal, R. Z. Legeros and K. A. Konsker, *J. Inorg. Biochem.*, 1990, **39**, 193.
21 J. W. P. Rothwell, J. S. Waugh and J. P. Yesinowski, *J. Am. Chem. Soc.*, 1980, **102**, 2637.
22 P. Li, K. Nakanishi, T. Kokubo and K. de Groot, *Biomaterials*, 1993, **14**, 963.

*Paper 8/03503B*